Cell Reports
Article

p53 DNA Binding Cooperativity Is Essential for Apoptosis and Tumor Suppression In Vivo

Oleg Timofeev,[1] Katharina Schlereth,[1] Michael Wanzel,[1] Attila Braun,[6] Bernhard Nieswandt,[6] Axel Pagenstecher,[2] Andreas Rosenwald,[7] Hans-Peter Elsässer,[3] and Thorsten Stiewe[1,4,5,*]
[1]Department of Molecular Oncology
[2]Department of Neuropathology
[3]Department of Cytobiology
[4]Universities of Giessen and Marburg Lung Center (UGMLC)
[5]German Center for Lung Research (DZL)
Philipps University, 35032 Marburg, Germany
[6]Department of Vascular Medicine, Rudolf Virchow Center for Experimental Biomedicine
[7]Institute of Pathology
University of Würzburg, 97080 Würzburg, Germany
*Correspondence: thorsten.stiewe@uni-marburg.de
http://dx.doi.org/10.1016/j.celrep.2013.04.008

SUMMARY

Four molecules of the tumor suppressor p53 assemble to cooperatively bind proapoptotic target genes. The structural basis for cooperativity consists of interactions between adjacent DNA binding domains. Mutations at the interaction interface that compromise cooperativity were identified in cancer patients, suggesting a requirement of cooperativity for tumor suppression. We report on an analysis of cooperativity mutant p53^{E177R} mice. Apoptotic functions of p53 triggered by DNA damage and oncogenes were abolished in these mice, whereas functions in cell-cycle control, senescence, metabolism, and antioxidant defense were retained and were sufficient to suppress development of spontaneous T cell lymphoma. Cooperativity mutant mice are nevertheless highly cancer prone and susceptible to different oncogene-induced tumors. Our data underscore the relevance of DNA binding cooperativity for p53-dependent apoptosis and tumor suppression and highlight cooperativity mutations as a class of p53 mutations that result in a selective loss of apoptotic functions due to an altered quaternary structure of the p53 tetramer.

INTRODUCTION

The p53 tumor-suppressor protein acts as a hub that integrates multiple intrinsic and extrinsic signals and launches a plethora of either cell-protective or cell-destructive programs in response to various types of cellular stress. Strong activation of p53 after acute genotoxic stress typically triggers cell destruction by apoptosis, whereas upon mild DNA damage, p53 acts cell protective by preferentially inducing damage repair and survival (Vousden and Prives, 2009). p53-dependent apoptosis serves as a major mechanism for counteracting hematologic malignancy (Schmitt et al., 2002), whereas other activities of p53, such as cell-cycle-inhibitory and prosenescent functions, are equally or even more relevant for suppression of other tumor types (Brady et al., 2011). Recent studies on restoration of p53 expression in transgenic mouse tumor models demonstrated that the spectrum of p53-triggered tumor-suppression programs depends strongly on oncogene and tissue context. Reactivation of the wild-type p53 protein in established Myc-driven B cell lymphomas led to tumor regression due to apoptosis (Martins et al., 2006; Ventura et al., 2007), whereas in sarcomas and hepatic carcinomas, p53 caused senescence-mediated cessation of tumor growth followed by tumor clearance through the innate immune system (Ventura et al., 2007; Xue et al., 2007). In addition, p53 has metabolic functions that regulate glucose uptake, glycolysis, oxidative phosphorylation, and reactive oxygen species (ROS) levels (Gottlieb and Vousden, 2010). Emerging evidence suggests that these metabolic functions of p53 contribute substantially to its tumor-suppressor activity and might in fact often be sufficient to counteract tumorigenesis (Li et al., 2012). Although a large amount of data about regulation of p53 turnover, transcriptional activity, posttranslational modifications, trafficking, and interaction with other proteins has been collected, it still remains poorly understood how p53 selects among the different cell-destructive or cell-protective programs to choose the mechanism that most efficiently prevents tumorigenesis (Beckerman and Prives, 2010; Schlereth et al., 2010b).

It was recently found that the four p53 molecules that assemble into the functional p53 tetramer engage in extensive intermolecular interactions when bound to a p53 response element on the DNA (Kitayner et al., 2006). Apart from the well-characterized interaction of the C-terminal oligomerization domains, these interactions involve the short H1 helix within the central DNA binding domain. H1 helix interactions are maintained by reciprocal salt bridges between oppositely charged glutamate (E180) and arginine (R181) residues (corresponding to E177 and R178 in the mouse) of each p53 monomer (Figure 1A). Functionally, these salt bridges were identified as the structural basis for the ability of p53 to bind DNA cooperatively

(Dehner et al., 2005; Schlereth et al., 2010a) and were shown to extend the target gene spectrum of p53 to include genes with noncanonical response elements that deviate from the consensus binding sequence (Schlereth et al., 2010a, 2010b). As a consequence, point mutations in codons 180 or 181 that reduce or increase H1 helix interactions (low or high DNA binding cooperativity mutations, respectively) modulate the transcriptional output of p53 signaling. Low cooperativity resulted in reduced binding of p53 to target promoters, in particular promoters of proapoptotic genes, whereas increased cooperativity led to excessive activation of apoptotic genes and elevated apoptotic activity (Schlereth et al., 2010a). Thus, although noncooperating p53 molecules are perfectly capable of arresting the cell cycle, induction of apoptosis requires p53 molecules to work together, suggestive of a safeguard mechanism designed to protect cells from careless killing through apoptosis.

Importantly, in contrast to classical hot spot mutations, cooperativity mutations do not affect residues that directly contact the DNA (class I mutations), and do not cause local or global unfolding of the p53 protein (class II mutations); therefore, they represent a functionally distinct class of p53 mutations (Dehner et al., 2005). Cooperativity-reducing mutations in codons 180 and 181 were detected in both sporadic tumors and in the germline of Li-Fraumeni patients who suffer from increased cancer susceptibility, suggesting that cooperativity is crucial for tumor suppression by p53. In this study we engineered the cooperativity-reducing mutation $p53^{E177R}$ in the mouse germline to explore the in vivo relevance of DNA binding cooperativity for tumor suppression.

RESULTS

Generation of Germline Cooperativity Mutant $p53^{E177R}$ Mice

In order to investigate the role of DNA binding cooperativity in vivo, we generated a mouse with the cooperativity-reducing point mutation $p53^{E177R}$ in the endogenous *Trp53* allele (Figure 1B). $p53^{E177R}$ is equivalent to human $p53^{E180R}$ and results in the replacement of negatively charged glutamic acid with positively charged arginine at codon 177. Mouse embryonic stem cells (ESCs) were electroporated with a targeting construct bearing the $p53^{E177R}$ mutation together with a puromycin resistance marker and a transcriptional stop sequence, flanked by loxP sites (lox-stop-lox [LSL] cassette; Olive et al., 2004). The LSL cassette introduced into the first intron allows conditional expression of the knockin allele by preventing p53 expression before Cre-mediated recombination occurs. After selection, resistant clones were tested for correct targeting by Southern blot (Figure 1C) and positive clones were injected into blastocysts. Chimeric animals were bred for germline transmission, which was confirmed by PCR genotyping using DNA isolated from tail tips (Figure 1D, upper panel). The presence of the point mutation was confirmed by sequencing (Figure 1E). The heterozygous F1 animals were mated with *Prm1-Cre* transgenic mice to remove the LSL cassette and generate the $Trp53^{E177R}$ allele. Excision of the LSL cassette was confirmed by PCR with tail-tip DNA (Figure 1D, lower panel). Hereafter, this allele is called RR to denote mutation of the H1 helix sequence from 177E;178R (ER, wild-type) to 177R;178R (RR, knockin). $p53^{+/RR}$ heterozygotes were intercrossed to obtain homozygous $p53^{RR/RR}$ animals, which were born at Mendelian ratio and had no growth retardation or obvious developmental defects (data not shown). Heterozygous $Trp53^{LSL\text{-}E177R}$ mice (called LSL-RR, representing a p53 null allele) were intercrossed to homozygosity to obtain a control cohort of p53-deficient mice ($p53^{-/-}$).

Cooperativity Mutant Mice Are Cancer Prone

To elucidate the role of DNA binding cooperativity in tumor suppression, we generated cohorts of mice with different p53 genotypes and monitored the animals for spontaneous tumor formation (Figure 1F). In compliance with published data (Donehower et al., 1992; Jacks et al., 1994), $p53^{-/-}$ mice showed early spontaneous tumorigenesis with a median survival of 131 days. Importantly, $p53^{RR/RR}$ mice were tumor prone, with a median overall survival of 361 days, whereas the lifespan of the $p53^{+/+}$ littermates exceeded 770 days. The heterozygous $p53^{+/-}$ and $p53^{+/RR}$ animals showed an intermediate lifespan of 438 and 587 days, respectively. Furthermore, $p53^{-/RR}$ mice with only one functional p53 knockin allele demonstrated a significantly shortened median survival (274 days). Taken together, these data clearly demonstrate that reduced DNA binding cooperativity compromises the ability of p53 to suppress spontaneous tumorigenesis.

Histopathology of the tumors showed that the tumor spectrum varied substantially among the different p53 genotypes. In line with literature data, ~90% of $p53^{-/-}$ mice developed lymphomas, which were predominantly of T cell origin (77% $B220^{-}CD3^{+}$), and only a few animals died from other tumors (e.g., teratocarcinomas; Figures 1G and 1H; Jacks et al., 1994). Interestingly, the percentage of hematological malignancy was markedly lower in the $p53^{RR/RR}$ cohort (59%), and only 30% of these neoplasias were $B220^{-}CD3^{+}$ and therefore diagnosed as T cell lymphoma (Figures 1G and 1H). Moreover, we frequently observed nonmalignant spleen hyperplasia in $p53^{RR/RR}$ mice, which was not the case for $p53^{-/-}$ animals (Figure 1I). Nonmalignant neoplasia was also rare in $p53^{+/-}$ and $p53^{-/RR}$ animals, whereas in $p53^{+/RR}$ mice, benign tumors were detected in 47% of cases (Figure 1I). We conclude that cooperativity mutants of p53 are less efficient in suppressing spontaneous tumorigenesis than wild-type p53 mice, resulting in substantial cancer susceptibility. However, compared with the p53 null allele, the cooperativity mutant p53 still provides a residual barrier against tumor development, protects against T cell lymphoma, and counteracts the transition from benign to malignant tumors.

Apoptosis Deficiency in Cooperativity Mutant Mice

Because DNA binding cooperativity was shown to be essential for transactivation of proapoptotic genes upon enforced expression of p53 in cell lines (Schlereth et al., 2010a), we expected to find apoptosis defects in $p53^{RR/RR}$ animals. When $p53^{+/+}$, $p53^{-/-}$, and $p53^{RR/RR}$ mice were exposed to whole-body γ irradiation (γ-IR), the acute DNA damage induced massive apoptosis in radiosensitive tissues of $p53^{+/+}$ animals, whereas $p53^{-/-}$ mice were apoptosis resistant as expected. In the thymus, developing cerebellum, and intestinal crypts of $p53^{RR/RR}$ animals, apoptosis levels were similarly low as in

Cell PRESS
Open ACCESS

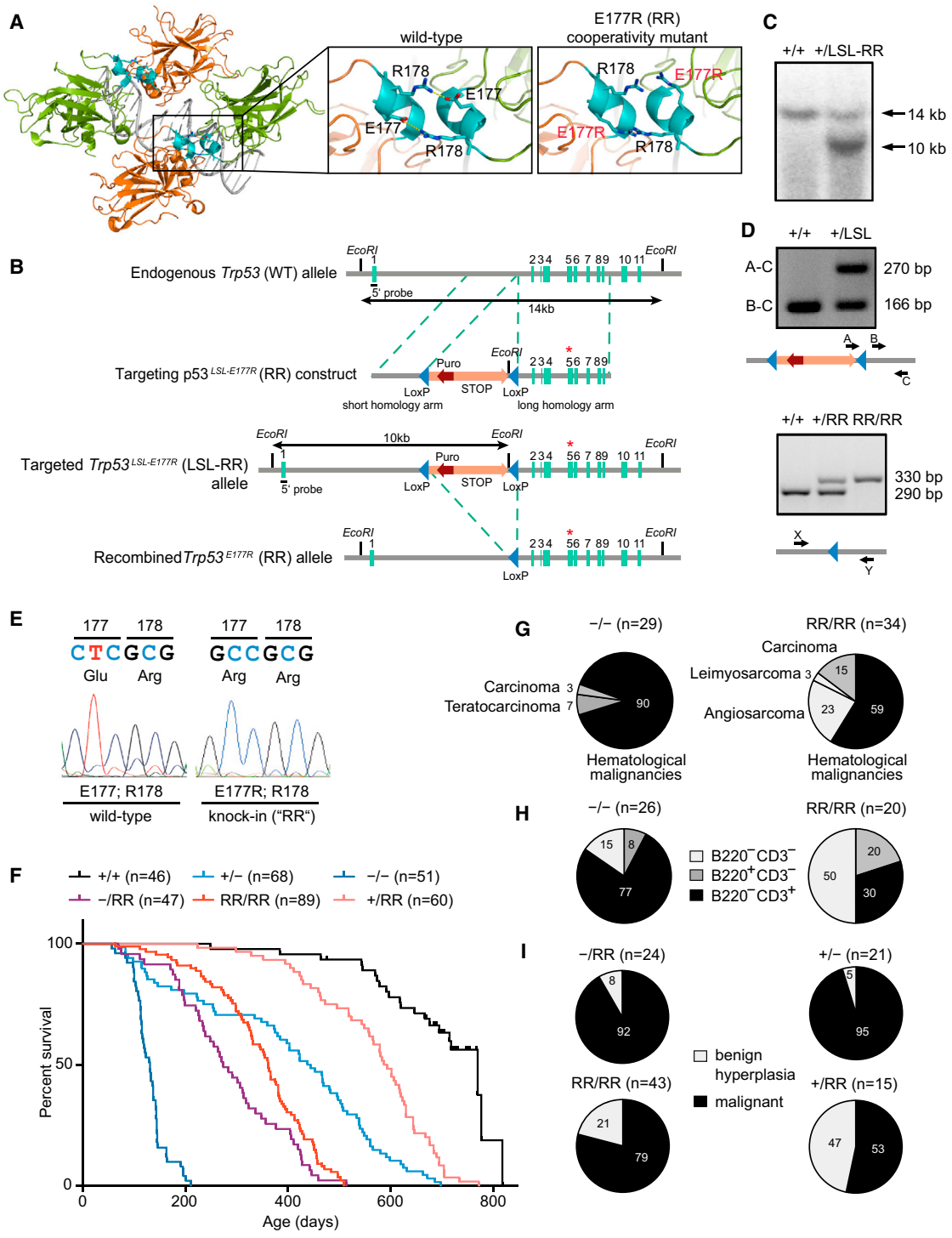

Figure 1. Generation of the p53^{E177R} Cooperativity Mutant Allele and Spontaneous Tumorigenesis

(A) Schematic representation of the p53 tetramer bound to DNA. Magnified views illustrate the H1 helix interactions in the p53 wild-type and p53^{E177R} mutant. H1 helices are highlighted in cyan; Glu180 and Arg181 are labeled.

(B) Targeting strategy. Asterisks mark the p53^{E177R} point mutation in exon 5.

(C) Identification of ESC clones with targeted integration of the p53^{E177R} construct by Southern blot. The 14 kb fragment corresponds to the wild-type, and the 10 kb fragment corresponds to the targeted *Trp53* allele.

(D) PCR amplification of conditional mutant alleles results in a 270 bp mutant product and a 166 bp control product. PCR primers flanking the site of recombination yield a 290 bp wild-type band and a 330 bp mutant p53 band.

(legend continued on next page)

p53 null mice 8 hr after IR (Figures 2A–2C). Moreover, excluding a simple delay, we observed no significant increase in the number of TUNEL-positive cells in intestinal crypts of $p53^{RR/RR}$ mice at different time points after IR (Figures 2C and 2D). Furthermore, when analyzing isolated thymocytes, which undergo a strictly p53-dependent apoptosis upon γ-IR (Clarke et al., 1993; Lowe et al., 1993b), we found that $p53^{RR/RR}$ thymocytes were as resistant to DNA-damage-induced apoptosis as the $p53^{-/-}$ ones (Figure 2E, left panel). Importantly, treatment with corticosteroids (1 μM dexamethasone) efficiently induced apoptosis in $p53^{RR/RR}$ thymocytes (Figure 2E, right panel), excluding p53-unrelated defects in the apoptotic signaling cascade.

To analyze the apoptosis deficiency of $p53^{RR/RR}$ mice in more detail, we sensitized mouse embryonic fibroblasts (MEFs) with different p53 genotypes to apoptosis induction by the adenoviral *E1A* oncogene (Lowe et al., 1993a). Again, in contrast to $p53^{+/+}$ MEFs, the $p53^{RR/RR}$ MEFs were as resistant to DNA-damage-induced apoptosis upon doxorubicin treatment as the $p53^{-/-}$ cells (Figure 2F). Likewise, no increase in caspase-3/7 activity or caspase-3 cleavage was observed in cooperativity mutant cells after treatment, although total p53 levels and serine 18-phosphorylation increased, indicative of normal p53 activation upon DNA damage (Figures 2F and 2G). In line with the notion that p53-dependent apoptosis relies on the transcriptional activation of proapoptotic target genes, *Puma* was only induced in p53 wild-type MEFs (Figure 2G). Likewise, *Puma*, *Noxa*, and *Bax* messenger RNA (mRNA) was only strongly upregulated in the thymus of irradiated $p53^{+/+}$ mice (Figure 2H). Thus, consistent with data from enforced p53 expression in cell culture, the DNA binding cooperativity of endogenous p53 also proved essential for transcriptional activation of multiple proapoptotic target genes and the acute apoptotic DNA damage response in vivo.

Apart from DNA-damage-induced apoptosis, p53-induced apoptosis is crucial to counteract the transforming activity of Myc (Hermeking and Eick, 1994). To investigate whether DNA binding cooperativity is essential for Myc-induced apoptosis, we analyzed MEFs of different p53 genotypes for apoptosis following activation of a tamoxifen-inducible Myc-ER allele. In contrast to $p53^{+/+}$ MEFs, the $p53^{RR/RR}$ MEFs and $p53^{-/-}$ cells were equally protected against Myc-induced apoptosis (Figure 2I). Moreover, $p53^{RR/RR}$ MEFs that were transduced with Myc formed multiple foci, albeit with lower frequency than the $p53^{-/-}$ cells (Figure 2J), hinting at other p53-dependent mechanisms that partially protect against transformation by Myc. We conclude that the DNA binding cooperativity of p53 is essential for apoptosis induction by Myc.

Reconstitution of DNA Binding Cooperativity Rescues the Apoptosis Defect

The $p53^{RR}$ mutant carries a bulky double-positive charge at the H1 helix that efficiently prevents H1 helix interactions and thus cooperative DNA binding. In principle, the same is observed for the $p53^{EE}$ mutant ($p53^{R178E}$, human $p53^{R181E}$), which is characterized by a strong double-negative charge. Interestingly, the combined expression of oppositely charged $p53^{RR}$ and $p53^{EE}$ was shown to enable the formation of mixed p53 tetramers that engage in cooperative, wild-type-like H1 helix interactions when binding to promoters of proapoptotic target genes (Figure 3A; Schlereth et al., 2010a). To prove that the apoptosis defect of the cooperativity mutant $p53^{RR}$ mouse is indeed a result of disrupted H1 helix interactions, we investigated whether apoptosis can be restored by complementation with $p53^{EE}$.

For this purpose, $p53^{+/+}$, $p53^{-/-}$, and $p53^{RR/RR}$ E1A-MEFs were infected with a lentivirus that labels the transduced cells with GFP and simultaneously allows tetracycline-inducible expression of $p53^{EE}$ (Figure 3B). Expression of $p53^{EE}$ had no or minimal effects on the percentage of GFP-positive $p53^{+/+}$ and $p53^{-/-}$ MEFs, respectively (Figure 3C), in line with the notion that $p53^{EE}$ has only a weak antiproliferative effect (Schlereth et al., 2010a). In contrast, $p53^{EE}$ strongly reduced the percentage of GFP-positive $p53^{RR/RR}$ MEFs, indicating that $p53^{EE}$ cooperates with $p53^{RR}$ to exert a potent antiproliferative effect. Furthermore, $p53^{EE}$ strongly sensitized $p53^{RR/RR}$ (but not $p53^{+/+}$ or $p53^{-/-}$) MEFs to a low dose of doxorubicin that on its own was insufficient to induce cell death in p53 wild-type MEFs (Figures 3D–3F). Importantly, $p53^{EE}$ rescued expression of the proapoptotic target genes *Puma*, *Noxa*, and *Bax* in a $p53^{RR}$-dependent manner (Figure 3G), resulting in rapid caspase-3 cleavage and high levels of cell death (Figures 3E and 3F). We conclude that $p53^{EE}$ expression completely rescues the apoptosis defect of $p53^{RR/RR}$ MEFs, proving that the failure to activate the apoptosis program is indeed a result of impaired H1 helix interactions and therefore reduced DNA binding cooperativity.

Senescence and Cell-Cycle Arrest in Cooperativity Mutant Mice

Besides apoptosis, p53 regulates other tumor-suppression pathways, such as cell-cycle arrest and senescence. To test whether these programs can be activated in $p53^{RR/RR}$ mice, we analyzed the proliferation of MEFs under the standard 3T3 protocol. Primary MEFs isolated from $p53^{RR/RR}$ embryos proliferated in culture slightly faster than $p53^{+/+}$ cells, but exhausted their replicative potential after six to eight passages (Figure 4A) and expressed senescence-associated β-galactosidase as a hallmark of cellular senescence similarly to $p53^{+/+}$ cells (Figure 4B). In response to doxorubicin-induced DNA damage, the percentage of bromodeoxyuridine (BrdU)-positive S phase cells decreased in $p53^{RR/RR}$ MEFs as a sign of cell-cycle arrest (Figure 4C). Moreover, DNA damage led to a robust transcriptional activation of p53 target genes involved in cell-cycle arrest, such as *Ccng1*, *Cdkn1a* (known as p21Cip1), and *Sfn* (14-3-3σ), as well as the negative regulator

(E) Sequence traces from p53 wild-type and $p53^{RR/RR}$ tail-tip DNA.
(F) Kaplan-Meier survival curves for mice of the indicated genotypes.
(G) Tumor spectrum diagnosed by histopathology.
(H) Hematological malignancies classified according to B220 and CD3 immunostaining.
(I) Proportion of benign hyperplasia and malignant neoplasia of the spleen.

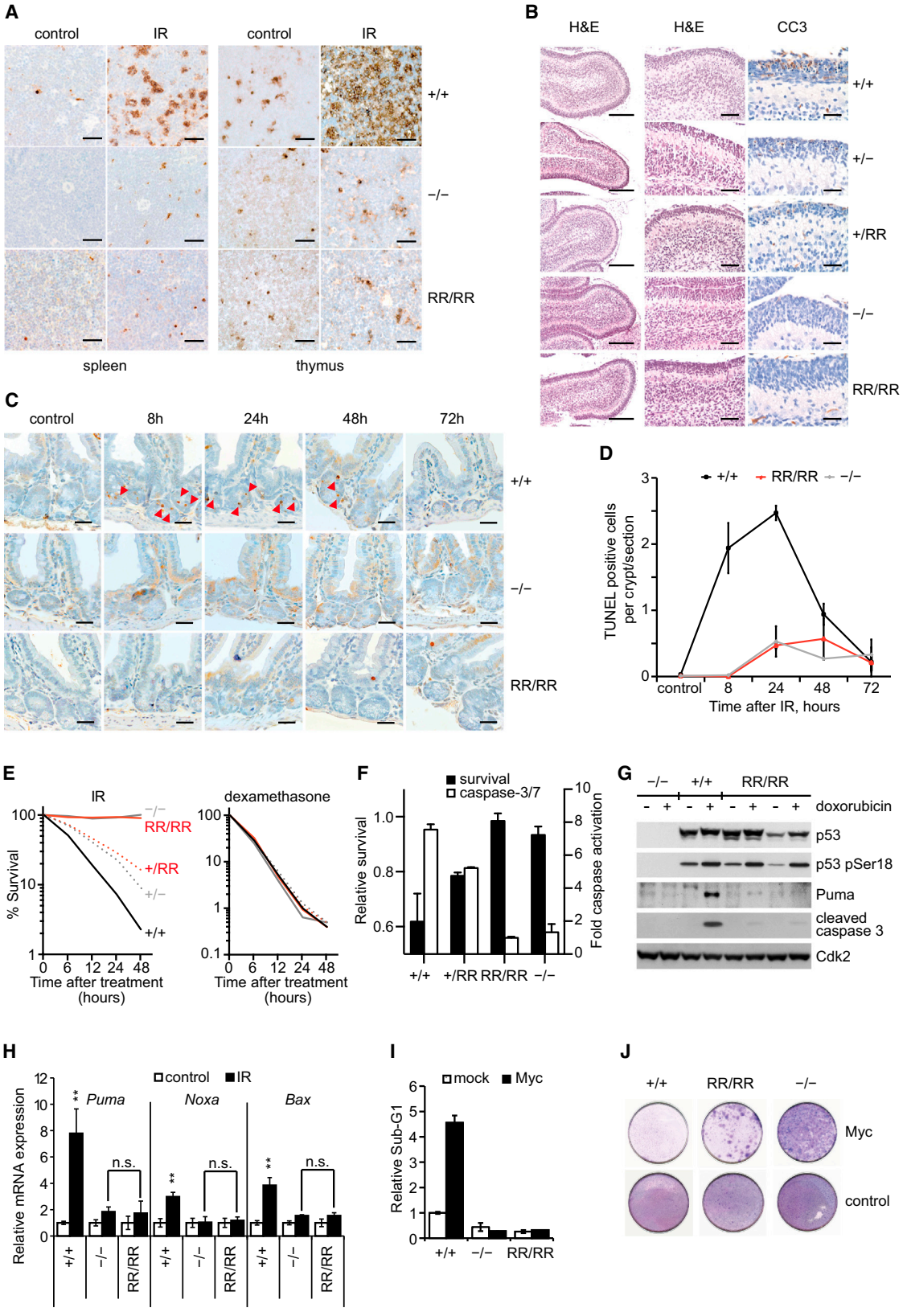

(legend on next page)

of p53, *Mdm2* (Figures 4D and 4E). Of note, target-gene activation and cell-cycle arrest in response to DNA damage appeared overall slightly lower in $p53^{RR/RR}$ than in $p53^{+/+}$ cells. To gain deeper insight into the cell-cycle functions of the $p53^{RR}$ mutant in vivo, we analyzed cell proliferation in response to whole-body γ-IR (Figures 4H and 4I). Acute DNA damage showed only weak effects on $p53^{-/-}$ mice, but resulted in a strong decrease in the number of proliferating cells with similar kinetics in intestinal crypts of $p53^{+/+}$ and $p53^{RR/RR}$ animals (Figures 4H and 4I).

In addition to DNA-damage-induced cell-cycle arrest, p53 is also responsible for cell-cycle withdrawal in response to other types of stress, including the expression of oncogenes (Serrano et al., 1997). Similarly to $p53^{+/+}$ MEFs, $p53^{RR/RR}$ cells showed premature, oncogene-induced senescence in response to $HRas^{G12V}$ (Figure 4F). In response to glucose deprivation, p53 is activated in an AMP-activated protein kinase (AMPK)-dependent manner and induces cell-cycle arrest and senescence (Jones et al., 2005). When treated with the AMPK activator 5-aminoimidazole-4-carboxamide (AICAR), $p53^{RR/RR}$ cells, like the $p53^{+/+}$ MEFs, arrested the cell cycle, whereas $p53^{-/-}$ cells continued to proliferate (Figure 4G). Collectively, our data indicate that the cooperativity mutant is capable of inducing cell-cycle arrest and senescence in response to p53 activation by DNA damage, oncogenes, and metabolic stress.

Antioxidant Metabolic Functions in Cooperativity Mutant Mice

The incidence of T cell lymphoma was markedly reduced in $p53^{RR/RR}$ mice compared with $p53^{-/-}$ animals (Figure 1H), indicating that $p53^{RR}$ retains functions important for suppressing this type of tumor. Since $p53^{RR/RR}$ mice are apoptosis-deficient in the thymus (Figures 2A and 2E), we investigated whether the cell-cycle-inhibitory senescence function of p53 limits thymic lymphoma development in $p53^{RR/RR}$ mice. However, we did not find any difference in senescence-associated β-galactosidase staining in thymus tissues collected from mice with different p53 status (data not shown), suggesting that neither p53's apoptotic activity nor its prosenescent activity—two responses that irreversibly remove the cell from the proliferative population—are relevant for protecting $p53^{RR/RR}$ mice from thymic lymphoma.

Interestingly, a number of recent studies have indicated that the ability of p53 to control tumorigenesis has a more subtle side, and in addition to eliminating the stressed cell, p53 can also play a role in the protection and survival of cells exposed to low, everyday levels of stress (Gottlieb and Vousden, 2010). Much of these cell-protective functions appear to rely on p53's potent ability to regulate key metabolic pathways, including oxidative phosphorylation and glycolysis, as well as several antioxidant defense pathways. In particular, development of T cell lymphoma in $p53^{-/-}$ mice was shown to be caused by increased oxidative DNA damage resulting from the accumulation of ROS, and could be prevented by continuous treatment with a ROS scavenger (Sablina et al., 2005). To explore this possibility, we analyzed ROS levels in thymocytes collected from young $p53^{+/+}$, $p53^{-/-}$, and $p53^{RR/RR}$ mice at 60–80 days of age, when lymphoma was not yet observed in $p53^{-/-}$ animals. ROS levels were significantly lower in the thymocytes of $p53^{+/+}$ and $p53^{RR/RR}$ mice than in $p53^{-/-}$ cells (Figure 5A). Consistently, the levels of the oxidative DNA adduct 8-hydroxy-2-deoxyguanosine (8-OHdG) were also markedly lower in both $p53^{RR/RR}$ and $p53^{+/+}$ samples than in the thymi of $p53^{-/-}$ mice (Figure 5B). p53 target genes that have been implicated in antioxidant protection, such as *Sesn1/2* (Sablina et al., 2005), *Aldh4* (Yoon et al., 2004), *Gls2* (Hu et al., 2010; Suzuki et al., 2010), and *Dram1* (a p53 target gene involved in autophagy; Crighton et al., 2006), were upregulated in a p53-dependent manner in doxorubicin-treated $p53^{RR/RR}$ MEFs, albeit at lower levels than in $p53^{+/+}$ cells (Figure 5D). Although *Tigar* and *Sco2* (p53 target genes that have been implicated in p53 regulation of glycolysis and oxidative phosphorylation; Bensaad et al., 2006; Matoba et al., 2006) were not p53 regulated in MEFs under our treatment conditions, both $p53^{RR/RR}$ and $p53^{+/+}$ MEFs showed lower glycolytic rates than $p53^{-/-}$ MEFs on the basis of extracellular acidification rate (ECAR) measurements obtained under both basal and glucose- or oligomycin-stimulated conditions (Figure 5C). $p53^{RR}$ therefore retains the ability of wild-type p53 to control glucose metabolism. Because inhibition of glycolysis by p53 diverts glucose flux into the pentose phosphate pathway to generate NADPH, which is needed for reduction of the ROS scavenger glutathione (Bensaad et al., 2006), the retained metabolic functions of $p53^{RR}$ provide an intriguing explanation for efficient suppression of thymic lymphoma in the absence of apoptosis and senescence.

Figure 2. Apoptosis Deficiency in Cooperativity Mutant Mice

(A) Representative TUNEL staining in the spleen and thymus of mice of the indicated genotypes either untreated (control) or 8 hr after 6 Gy of γ-IR. Scale bars: 25 μm.

(B) Apoptosis detected using antibodies specific for activated (cleaved) caspase-3 (CC3) in the cerebellum of 5-day-old γ-irradiated (6 Gy) mice. Scale bars: 100 μm, 50 μm, and 25 μm (left to right).

(C and D) TUNEL staining in the small intestine of mice sacrificed at 8, 24, 48, and 72 hr after γ-IR (6 Gy). TUNEL-positive cells were counted in 50 half-crypts (one section per mouse). Data represent mean ± SD. Scale bars: 25 μm.

(E) Viability of primary thymocytes after ex vivo γ-IR (6 Gy) or dexamethasone treatment (1 μM). Data represent mean ± SE.

(F) Viability and caspase-3 activity of E1A-immortalized MEFs 24 hr after treatment with 0.4 μg/ml doxorubicin. Data represent mean ± SD.

(G) Immunoblot analysis for the indicated proteins in E1A-immortalized MEFs 16 hr after treatment with 2 μg/ml doxorubicin. Cdk2 serves as a loading control. Two independent $p53^{RR/RR}$ MEF preparations are shown.

(H) Quantitative RT-PCR (qRT-PCR) analysis of the indicated mRNAs in the thymus of mice either untreated (control) or 8 hr after 6 Gy of γ-IR. Shown are relative (mean ± SD) mRNA expression levels normalized to β-actin and untreated samples. $^{**}p < 0.01$, Mann-Whitney test.

(I) Apoptosis (detected as sub-G1 population) in primary MEFs 48 hr after Myc expression. Error bars indicate SD.

(J) Colony formation assay of primary MEFs expressing Myc.

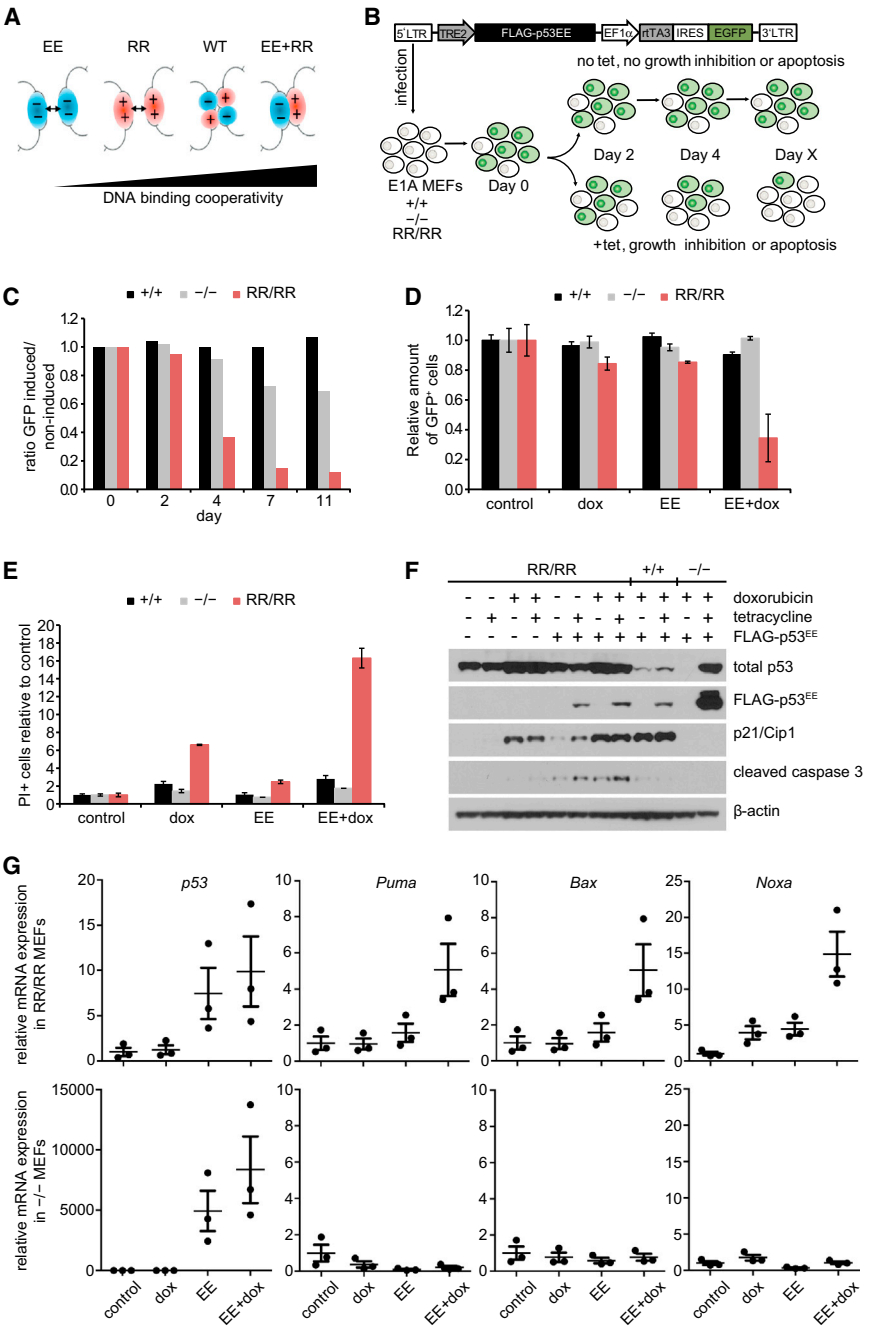

Figure 3. Reconstitution of DNA Binding Cooperativity Rescues the Apoptosis Defect

(A) Rescue of DNA binding cooperativity by complementation with the p53^{R178E} (EE) mutant.
(B–E) Apoptosis rescue experiment.
(B) Schematic overview.
(C) Percentage of GFP$^+$ cells following tet-induced EE expression relative to noninduced controls.
(D) Percentage of GFP$^+$ cells 12 hr following induction of EE ± doxorubicin treatment (0.2 μg/ml) relative to untreated cells.
(E) PI$^+$ dead cells treated as in (D) were quantified by fluorescence-activated cell sorting (FACS).
(F) Immunoblot analysis of lysates prepared from E1A-immortalized MEFs transduced as indicated with the tet-inducible FLAG-p53^{EE} expression construct and treated with 0.2 μg/ml doxorubicin ± 1 μg/ml doxycycline (tet) for 12 hr.
(G) qRT-PCR analysis of *p53*, *Puma*, *Bax*, and *Noxa* mRNA expression 12 hr following treatment with 0.4 μg/ml doxorubicin ± tet. Data were normalized to β-actin and untreated controls.
All data are presented as mean ± SD.

Tumor Suppression by p53^{RR} Is Dependent on Oncogene Context

Together, our data indicate that the p53^{RR} mutant is apoptosis incompetent but retains other tumor-suppression activities, such as induction of cell-cycle arrest and senescence, protection from oxidative stress, and regulation of metabolism. Although the nonapoptotic, antioxidant activity explains how p53^{RR} prevents thymic lymphomagenesis, we predicted that, due to its apoptosis deficiency, p53^{RR} might be inefficient at suppressing tumorigenesis under conditions in which apoptosis represents the major barrier to tumor development. To explore this possibility, we used a transplantable fibrosarcoma model in which p53-dependent apoptosis was shown to be important for suppression of tumor growth and chemotherapy response (Lowe et al., 1993a, 1994). Primary MEFs isolated from p53$^{+/+}$, p53$^{-/-}$, and p53$^{RR/RR}$ embryos were infected with retroviruses bearing *E1A* and *HRas*^{G12V} oncogenes and after selection were injected subcutaneously into immunodeficient nude mice to induce fibrosarcomas. We observed significantly increased tumor growth from both p53$^{-/-}$ and p53$^{RR/RR}$ cells compared with p53$^{+/+}$ MEFs (Figure 6A). Furthermore, in stark contrast to p53$^{+/+}$ xenografts, no increase in apoptosis was detected in p53$^{RR/RR}$ tumors after chemotherapy (Figure 6B). Thus, apoptosis deficiency completely abrogated the tumor-suppressor activity of the p53^{RR} mutant in this transplanted fibrosarcoma model.

To investigate whether p53^{RR} can suppress tumorigenesis in a genetically defined, nontransplanted mouse tumor model, we used *Eμ-Myc* mice that mimic aggressive Burkitt-like B cell lymphomas in humans (Adams et al., 1985). In *Eμ-Myc* lymphomas, apoptosis is considered to be essential for tumor suppression by p53 (Michalak et al., 2008; Schmitt et al., 2002). We generated cohorts of *Eμ-Myc* mice with different p53 genotypes and monitored tumorigenesis in these mice. We observed a strongly reduced survival of p53$^{+/RR}$ mice in comparison with their p53$^{+/+}$ littermates (Figure 6C).

Genotyping of tumor samples showed a loss of the p53 wild-type allele in most tumor samples from $p53^{+/-}$ and $p53^{+/RR}$ mice, indicating selection against wild-type p53 in favor of either the p53 null or the apoptosis-deficient $p53^{RR}$ allele (Figure 6D). Strong nuclear p53 staining in $p53^{-/RR}$ lymphomas indicates that $p53^{RR}$ is expressed but is unable to counteract tumor growth efficiently (Figure 6E). These data support the notion that p53-dependent apoptosis is essential for suppression of Myc-driven B cell lymphomagenesis.

Interestingly, the median survival of $p53^{+/RR}$ mice was ~10 days longer than that of $p53^{+/-}$ mice ($p < 0.0001$), suggesting that $p53^{RR}$ retains residual tumor-suppressor activity that delays lymphomagenesis in this model. Histological analysis of tumors showed low levels of spontaneous apoptosis in all but the $p53^{+/+}$ mice and excludes a residual apoptotic activity as an explanation (Figures 6E and 6F). However, lymphomas from $p53^{+/RR}$ mice displayed high amounts of senescent cells, similar to or higher than the amounts observed in tumors from $p53^{+/+}$ animals (Figures 6E and 6F). It was previously reported that p53-induced apoptosis of lymphoma cells can trigger macrophages to secrete transforming growth factor β (TGF-β) as a critical non-cell-autonomous inducer of cellular senescence (Reimann et al., 2010). However, both apoptosis levels and macrophage infiltration were found to be low in lymphomas of $p53^{+/RR}$ mice (Figures 6E and 6F), indicating that senescence in these lymphomas is instead mediated by a cell-autonomous mechanism that is directly triggered by p53 in the absence of apoptotic functions.

In summary, the residual, nonapoptotic tumor-suppressor activities of p53 appear sufficient to protect against tumors such as thymic lymphoma, but p53-induced apoptosis, which relies on cooperative DNA binding by several p53 molecules, is indispensable for suppressing other oncogene-induced tumors.

DISCUSSION

p53 DNA binding cooperativity mutations represent a distinct class of p53 mutations. These mutations affect interactions between adjacent p53 DNA binding domains in the tetrameric p53-DNA complex, but, unlike typical class I or II hot spot mutations, they do not disturb folding, tetramerization, or DNA contact (Dehner et al., 2005; Schlereth et al., 2010a). Nevertheless, cooperativity mutations have been identified in sporadic tumors and segregate with cancer susceptibility in Li-Fraumeni syndrome families, which implies a central role for p53 DNA binding cooperativity in tumor suppression (Schlereth et al., 2010a). Here, we provide unequivocal genetic in vivo evidence supporting this notion.

We observed a strikingly increased incidence of spontaneous tumorigenesis that resulted in reduced survival in mice with the cooperativity-reducing point mutation $p53^{RR}$ (Figure 1F). Furthermore, the $p53^{RR}$ mutant could not suppress the growth of oncogene-induced xenograft tumors and did not pose a substantial barrier to Myc-driven lymphomagenesis (Figure 6). Our studies showed that the cooperativity mutation abrogated p53-mediated transactivation of key proapoptotic target genes, including *Puma*, *Noxa*, and *Bax*, resulting in apoptosis resistance in response to acute genotoxic stress or Myc overexpression. Importantly, the apoptosis defect could be fully rescued with a second cooperativity mutant that complemented the $p53^{RR}$ mutant and restored cooperativity, thereby proving that a lack of cooperativity is the underlying cause of apoptosis resistance. Apoptosis-independent activities of p53, such as cell-cycle arrest, senescence, regulation of metabolism, and antioxidant functions, were retained in $p53^{RR}$ mice. Interestingly, these p53 functions were largely sufficient to protect against spontaneous T cell lymphomas, indicating that in spite of their reduced potency, cooperativity mutants can provide residual tumor suppression depending on the tissue and oncogene context.

For a long time, elimination of damaged cells by apoptosis seemed to be the safest way to prevent tumorigenesis, and thus p53's proapoptotic activity was considered to be of crucial importance for tumor suppression (Lowe et al., 1993a, 1994). This notion is supported by the fact that disruption of apoptosis downstream of p53 eliminates the pressure to inactivate p53 during Myc-driven lymphomagenesis, indicating that apoptosis is the only p53 function that is selected against (Schmitt et al., 2002). Conversely, a mutant of p53 in the proline-rich region, which is deficient in cell-cycle arrest functions but retains proapoptotic activity, reduces spontaneous tumorigenesis in gene-modified mice (Toledo et al., 2006). Similarly, mice deficient for *Cdkn1a* (p21CIP1), which mediates p53-induced cell-cycle arrest and contributes to the development of cellular senescence, do not show the cancer susceptibility of p53-deficient animals (Deng et al., 1995).

However, recent data provide evidence that apoptosis may be dispensable for p53's tumor-suppressor activity. The absence of spontaneous tumors in mice lacking *Puma*, a p53 target gene that is crucial for p53-mediated apoptosis in several tissues (Jeffers et al., 2003), suggests that p53 can provide sufficient tumor suppression in the absence of apoptosis (Michalak et al., 2008). Apart from apoptosis, p53 is well characterized for inducing senescence in response to persistent low-level activation of DNA damage signaling upon expression of oncogenes such as Ras (Serrano et al., 1997). p53-triggered senescence was also readily detected in premalignant tumors initiated by conditional expression of oncogenic $Kras^{G12V}$ in mice and protected against progression to carcinomas (Collado et al., 2005). Moreover, a number of apoptosis-deficient p53 mutants have recently been characterized in transgenic mouse models. For example, an apoptosis defect was reported for mice with a mutation to proline at arginine-172, which is crucial for coordinating the central zinc ion and stabilizing the overall structure of the DNA binding domain (Liu et al., 2004). $p53^{R172H}$, one of the most common hot spot mutations, causes a global denaturation of the DNA binding domain associated with complete loss of function (Bullock and Fersht, 2001). Although it has not been proved experimentally, the $p53^{R172P}$ mutation may have a more subtle effect that selectively destabilizes the H1 helix and thus compromises DNA binding cooperativity in a manner similar to that observed for the $p53^{RR}$ mutation. Importantly, although the $p53^{R172P}$ mutant is apoptosis deficient, it was shown to suppress spontaneous tumorigenesis and maintain genomic stability due to its intact cell-cycle arrest and senescence functions (Cosme-Blanco et al., 2007; Liu et al., 2004; Van Nguyen et al., 2007). Similarly, the transactivation-domain mutant

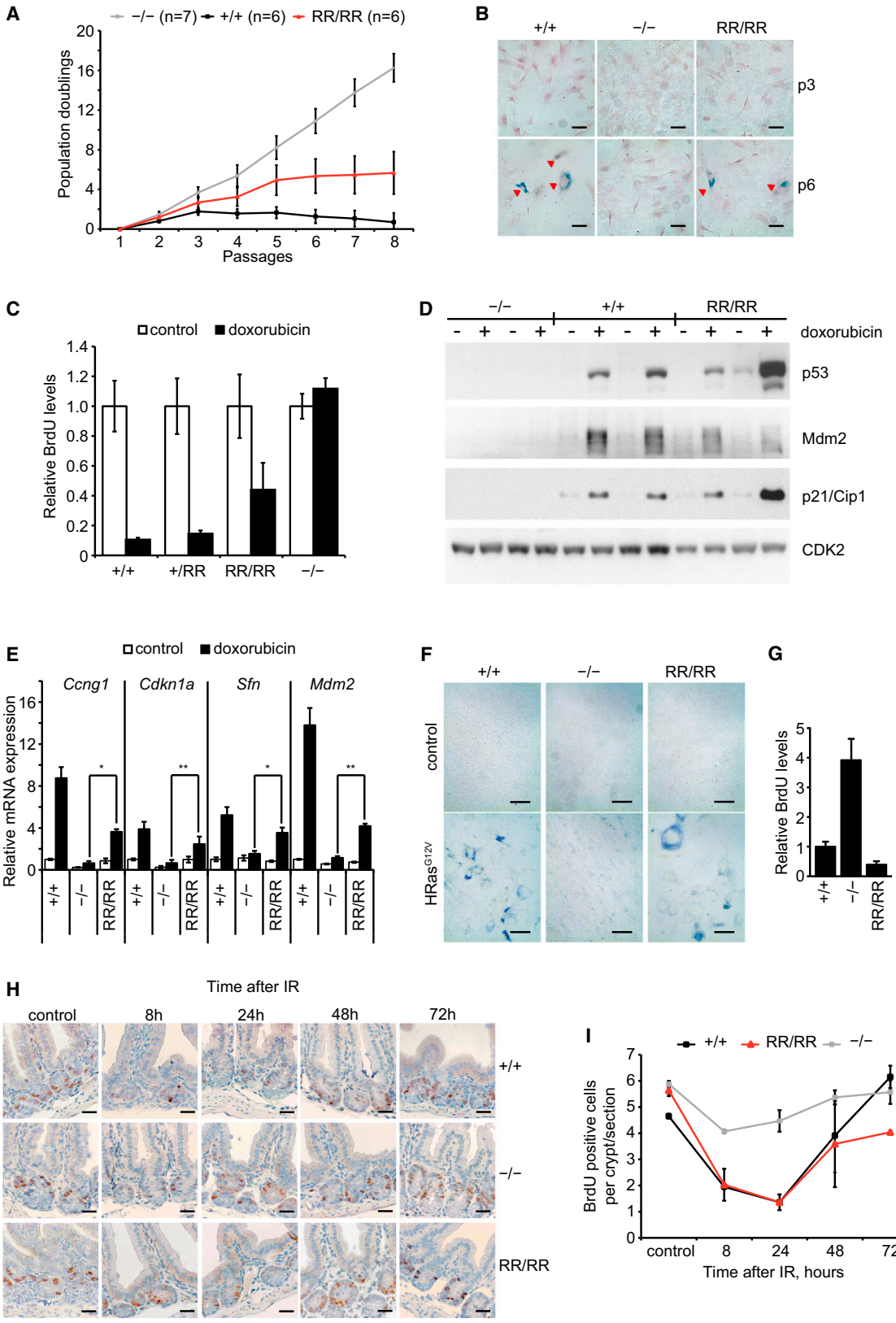

(legend on next page)

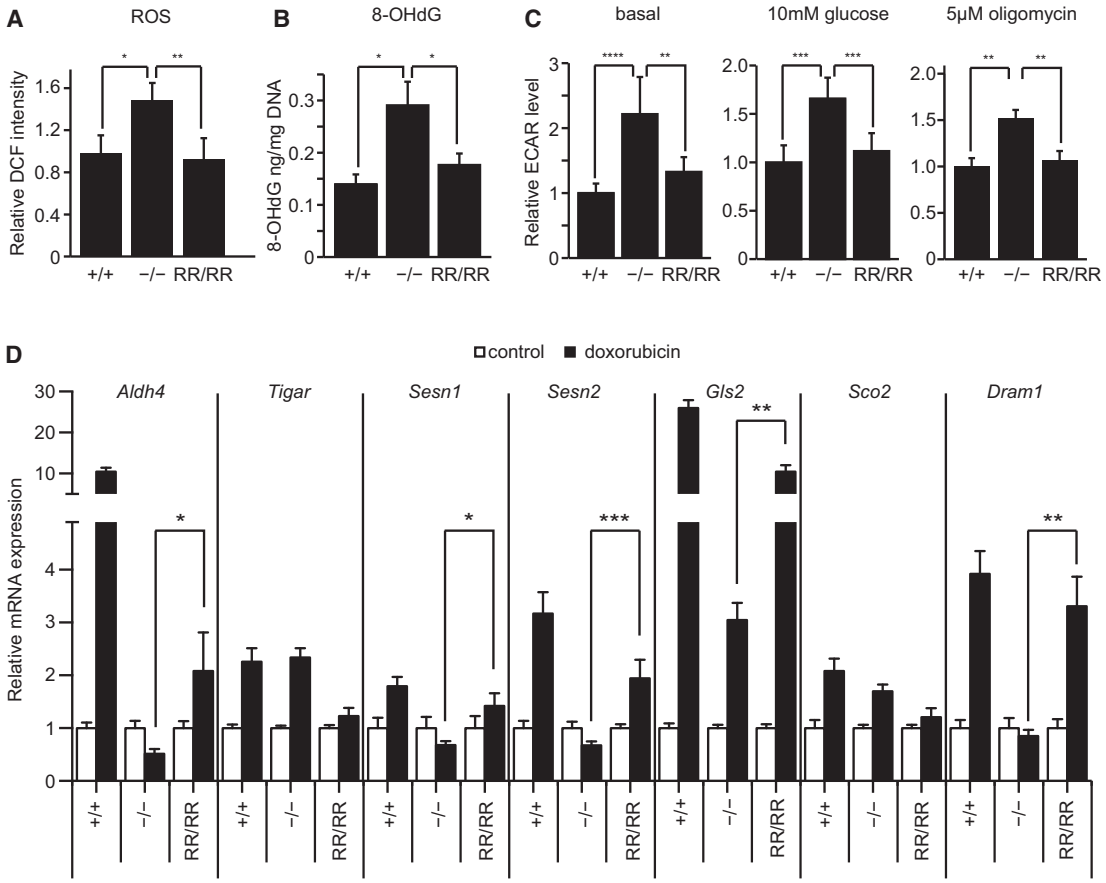

Figure 5. Antioxidant Metabolic Functions in Cooperativity Mutant Mice

(A) ROS levels in thymocytes from 60- to 80-day-old mice assessed by flow-cytometric 5-(and-6)-chloromethyl-2′,7′-dichlorodihydrofluorescein diacetate (DCF) staining normalized to $p53^{+/+}$ samples. *p < 0.05; **p < 0.01 Mann-Whitney test.

(B) Detection of oxidation-induced DNA damage in thymi by measurement of 8-OHdG in genomic DNA samples. *p < 0.05, Mann-Whitney test.

(C) ECAR as a measure of glycolytic activity measured in primary MEFs in the absence of glucose (basal), after stimulation with 10 mM glucose, and after inhibition of aerobic respiration by oligomycin. **p < 0.005; ***p < 0.001; ****p < 0.0001, Mann-Whitney test.

(D) qRT-PCR analysis of mRNA expression levels in primary MEFs treated as indicated for 12 hr with 0.4 μg/ml doxorubicin. Data were normalized to β-actin and untreated controls.

All data show mean ± SD. Statistical analysis: *p < 0.05; **p < 0.005; ***p < 0.001, Mann-Whitney test.

$p53^{L25Q;W26S}$, which is deficient for transcriptional activation of most apoptotic and cell-cycle arrest target genes but nevertheless is proficient in senescence induction, suppressed $Kras^{G12D}$-driven lung tumorigenesis, indicating that full transcriptional activity is not required for the prosenescent functions of p53 (Brady et al., 2011). Our study of the cooperativity mutant $p53^{RR}$, which has a severely compromised DNA binding ability and a strongly reduced target gene spectrum, provides evidence in support of this notion. Although $p53^{RR}$ was unable to induce apoptosis in response to DNA damage or oncogenes, it

Figure 4. Senescence and Cell-Cycle Arrest in Cooperativity Mutant Mice

(A) Proliferation potential of primary MEFs under the 3T3 protocol.

(B) Senescence-associated β-galactosidase in primary MEFs from (A). Scale bars: 25 μm.

(C) BrdU positivity in cells treated for 12 hr with doxorubicin (0.2 μg/ml) relative to untreated controls.

(D) Immunoblot analysis of primary MEFs treated as indicated with 0.4 μg/ml doxorubicin for 24 hr. Cdk2 serves as a loading control. Two independent MEF preparations are shown for each genotype.

(E) qRT-PCR analysis of mRNA expression levels in primary MEFs treated as indicated for 12 hr with 0.4 μg/ml doxorubicin. Data were normalized to β-actin and untreated controls. *p < 0.05; **p < 0.01; Mann-Whitney test.

(F) Senescence-associated β-galactosidase in MEFs transduced with empty vector or $HRas^{G12V}$.

(G) BrdU incorporation in primary MEFs treated with the AMPK activator AICAR (0.5 mM) relative to untreated controls.

(H) BrdU staining in intestine at the indicated time points after whole-body γ-IR (6 Gy).

(I) Quantification of $BrdU^+$ S phase cells.

All data show mean ± SD. Scale bars represent 20 μm.

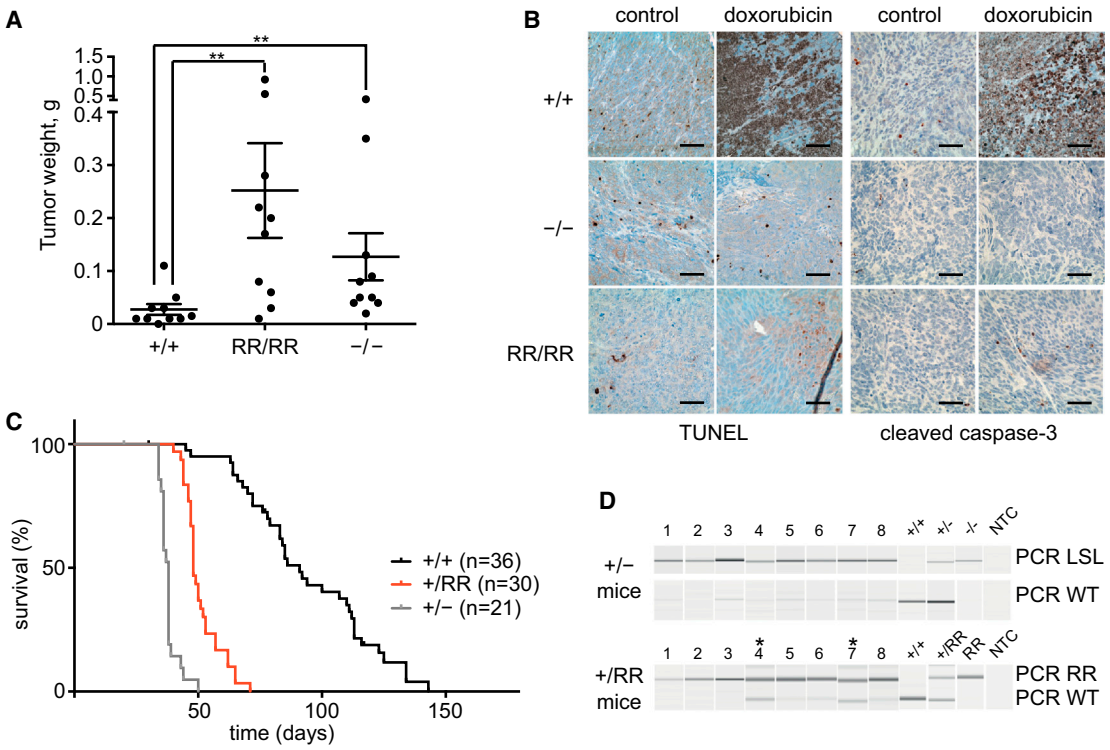

(legend on next page)

established a cell-cycle arrest after DNA damage and drove MEFs into senescence upon cell-culture stress or expression of oncogenic *Ras*.

Recent data suggest that both cell-autonomous and non-cell-autonomous senescence can be relevant for suppression of hematological malignancies. In *Eμ-Myc;Trp53*$^{+/+}$ mice, apoptotic cells attract and activate macrophages to secrete TGF-β, which induces senescence in a non-cell-autonomous manner. Inactivation of the senescence-related histone methyltransferase *Suv39h1* abrogated cellular senescence and significantly accelerated lymphoma development, indicating that p53-dependent apoptosis can trigger a tumor stroma-derived senescence response that limits Myc-driven lymphomagenesis (Reimann et al., 2010). In our experiments, *Eμ-Myc*-induced lymphomagenesis in p53$^{+/RR}$ mice was significantly delayed by ~10 days compared with p53$^{+/-}$ animals concomitantly with high levels of senescence in the lymphoma cells (Figure 6E). However, this occurred in the absence of elevated levels of apoptosis and was not accompanied by recruitment of macrophages or increased secretion of TGF-β (data not shown), suggesting that senescent lymphoma cells in p53$^{+/RR}$ mice are a consequence of the documented cell-autonomous, DNA-damage-response-mediated, prosenescent capability of Myc (Reimann et al., 2010).

Genome-wide transcriptional and chromatin profiling is generating a constantly growing list of p53 target genes, many of which are not linked directly to either apoptosis or senescence. Among them are genes that participate in the regulation of energy metabolism, autophagy, and antioxidant defense (Gottlieb and Vousden, 2010). These alternative p53-dependent pathways, which promote homeostatic stability in response to metabolic stress such as glucose starvation or ROS exposure, are believed to contribute substantially to tumor suppression (Li et al., 2012). For example, p53-induction of *TIGAR* inhibits glycolysis and diverts glucose flux into the pentose phosphate pathway to increase NADPH-dependent glutathione reduction (Bensaad et al., 2006). Furthermore, p53 directly transactivates genes such as *Sesn1* and *Sesn2* (Sablina et al., 2005), *Gls2* (Hu et al., 2010; Suzuki et al., 2010), and *Aldh4* (Yoon et al., 2004), all of which contribute to the antioxidant defense. In line with the notion that p53 is a central regulator of ROS metabolism, loss of p53 leads to oxidative DNA damage, a major cause of thymic lymphoma in p53$^{-/-}$ mice (Sablina et al., 2005). The p53^{RR} mutant retained the ability to upregulate antioxidant genes and inhibit glycolysis (Figure 5). This resulted in low, p53 wild-type-like ROS and oxidative DNA-damage levels in p53$^{RR/RR}$ thymi and concomitantly a low incidence of thymic lymphoma. Thus, our data support the relevance of alternative p53-regulated effector programs, such as regulation of glucose metabolism and ROS levels, for tumor suppression.

Considering that cooperativity mutants bind and regulate only a limited set of all wild-type p53 target genes (Schlereth et al., 2010a), it is surprising that the remaining small number of target genes proved sufficient to maintain at least partially the cell-cycle arrest, senescence, antioxidant, and metabolic functions of p53, effectively counteract the transforming activity of Ras (Figure 4F), and limit the spontaneous development of T cell lymphoma in mice (Figure 1H). Similarly, the recently reported p53^{3KR} mutant, which eliminates three acetylation sites in the DNA binding domain, lacks the three major p53 tumor suppressor activities (apoptosis, cell-cycle arrest, and senescence) but retains residual antioxidant and metabolic functions sufficient to delay thymic lymphomagenesis (Li et al., 2012). Likewise, the p53^{25,26} transactivation domain mutant, which is severely compromised for transactivation of most p53 target genes, retains the ability to induce senescence and suppress tumorigenesis in multiple tumor models (Brady et al., 2011; Jiang et al., 2011). Because cooperativity, acetylation, and transactivation-domain mutations target different aspects of p53-mediated gene regulation, the changes in p53's target gene spectrum are dissimilar. For example, although p53^{3KR} does not activate *Cdkn1a*, *Puma*, *Noxa*, or *Bax*, p53^{25,26} and p53^{RR} retain the ability to activate *Bax* and *Cdkn1a*, respectively. Different target genes therefore exhibit distinct requirements for p53 acetylation, DNA binding, and transactivation. Which specific sets of p53 target genes are the most relevant for tumor suppression in different oncogenic and cellular signaling contexts remains to be elucidated. It is anticipated that cooperativity mutant mice will provide a valuable tool for such studies.

It is unknown whether DNA binding cooperativity of p53 is regulated in vivo, but this mechanism might provide a tempting opportunity for the development of new strategies to modulate the p53 response to chemotherapy. "Sensitization" of the p53 pathways by extra genomic copies of p53 or dampening of negative regulators such as *Wip1* inhibits tumor growth and leads to a cancer-resistant phenotype in mice (Demidov et al., 2007; García-Cao et al., 2002; Shreeram et al., 2006). One can suppose that enhanced DNA binding cooperativity would sensitize cells to oncogenic stress, thus providing protection against spontaneous tumorigenesis in patients with a predisposition to familial cancer. We have shown that higher than normal cooperativity, achieved experimentally by coexpressing the two complementing cooperativity mutants p53^{RR} and p53^{EE}, results in cell death

Figure 6. Tumor Suppression by p53^{RR} Is Dependent on Oncogene Context

(A and B) p53^{RR} is a poor suppressor of fibrosarcoma xenografts. Primary MEFs were transformed with E1A and HRas^{G12V} and injected subcutaneously into nude mice.

(A) Mean (±SD) weight of xenograft tumors after 2 weeks. **$p < 0.001$, Mann-Whitney test.

(B) Apoptosis detected by TUNEL or cleaved caspase-3 staining treated as indicated for 24 hr with 20 mg/kg doxorubicin. Scale bars: 50 μm.

(C–F) p53^{RR} is a poor suppressor of *Eμ-Myc* lymphomas.

(C) Kaplan-Meier survival curves of *Eμ-Myc* mice of the indicated p53 genotypes. $p < 0.0001$ for all pairwise comparisons (log rank test).

(D) Loss of heterozygosity (LOH) analysis by PCR genotyping of *Eμ-Myc* lymphomas. Asterisks mark lymphoma samples without LOH.

(E) Histological analysis for p53, markers of apoptosis (TUNEL, cleaved caspase-3), macrophages (F4/80), and senescence (senescence-associated β-galactosidase, H3K9me3) in representative lymphomas from mice of the indicated p53 genotypes. Scale bars: 50 μm.

(F) Quantification of histological analyses in (E). At least 26 sections from >10 mice of each genotype were analyzed. Shown is the distribution of staining intensity scores among the samples for each p53 genotype. ***$p < 0.0005$; ****$p < 0.0001$, unpaired t test.

at doses of doxorubicin that are inefficient for killing p53 wild-type cells (Figures 3D–3F). Increasing cooperativity with small molecules might therefore represent an attractive and straightforward way to enhance the proapoptotic activity and simultaneously reduce the prosurvival activity of p53. Although they would clearly be beneficial for patients with wild-type p53, such strategies might also prove helpful for cooperativity mutants of p53 and possibly for reactivating the more common p53 hot-spot mutants. However, considering conflicting reports on premature aging as a possible consequence of increased p53 activity (Reinhardt and Schumacher, 2012), caution is warranted because it is unknown at present what consequences an increase in DNA binding cooperativity would have for normal cells and in particular stem cells.

On the other hand, the extent to which the nonapoptotic functions of p53 contribute to the effectiveness of treatment and suppression of residual disease is unclear. p53-triggered senescence in combination with clearance of senescent tumor cells by the immune system might provide protection against relapse similar to that achieved by direct killing (Xue et al., 2007), whereas extensive apoptosis induced by aggressive cytotoxic therapy often burdens patients with severe side effects. Moreover, there is evidence that p53-induced apoptosis might even actively drive tumor formation, whereas mice defective in p53-induced apoptosis due to loss of its proapoptotic target gene, *Puma*, resist γ-IR-induced lymphomagenesis (Labi et al., 2010). This indicates that modulating p53 activity to reduce apoptosis while retaining other tumor-suppression functions, as could be achieved by reducing cooperativity, might be useful for designing therapies with less side effects.

We believe that our data contribute to a deeper understanding of the mechanisms that regulate p53-mediated cell-fate decisions because they indicate an essential requirement of p53 cooperativity for apoptosis induction as the strongest outcome of p53 pathway activation. The demonstrated tissue- and context-dependent role of p53 cooperativity for tumor suppression will pave the way for designing strategies aimed at modulating p53 cooperativity to fine-tune p53 activity for improved cancer therapy.

EXPERIMENTAL PROCEDURES

Generation and Characterization of Mice

For generation of the *Trp53*^{R177E} knockin mouse, the targeting vector (Olive et al., 2004) was modified to carry only the mutation CTC->GCC in exon 5 of *Trp53*, resulting in a Glu->Arg substitution at codon 177. The point mutation was introduced using the QuikChange Multi Site-Directed Mutagenesis Kit (Stratagene) and the primer 5′-GAGGTCGTGAGACGCTGCCCCCACCATC GGCGCTGCTCCGATGG-3′. The complete targeting vector was verified by Sanger sequencing. R1 mouse ESCs (129X1/SvJ × 129S1) were electroporated with the targeting construct linearized by NotI. Selection was performed in the presence of 2 μg/ml puromycin, and resistant clones were tested using Southern blot with EcoRI-digested genomic DNA according to the standard protocol. A 5′ external probe and an internal probe (complementary DNA [cDNA] from puromycin marker) were amplified by PCR and used for identification of correctly targeted clones. Twenty out of 480 ESC clones were confirmed to be positive for targeted integration. Twelve clones were confirmed for the presence of the mutation by sequencing of PCR products obtained from exons 5 and 6 using genomic DNA isolated from ESCs (primers: F-5′-TCTCTTCCAGTACTCTCCTCC-3′ and R-5′-AATTACAGACCTCGGGT GGCT-3′). Germline transmission was achieved with two clones used for blastocyst injection. Additional mutations were excluded by sequencing of all exons and exon-intron boundaries in the *Trp53* gene. Knockin mice were kept on a pure 129Sv background. *Prm1-Cre* and *Eμ-Myc* mice were obtained from The Jackson Laboratory. All experiments were performed in accordance with the German Animal Welfare Act (Deutsches Tierschutzgesetz) and were approved by the local authorities.

For further details regarding the materials and methods used in this work, see Extended Experimental Procedures.

SUPPLEMENTAL INFORMATION

Supplemental Information includes Extended Experimental Procedures and can be found with this article online at http://dx.doi.org/10.1016/j.celrep.2013.04.008.

LICENSING INFORMATION

ACKNOWLEDGMENTS

We thank T. Jacks for providing the targeting construct. We also thank S. Bischofsberger and A. Grzeschiczek for excellent technical assistance, and current and former members of the Stiewe laboratory for advice and critical review of the manuscript. T.S. acknowledges support from the DFG (TR17, TR81, and KFO 210), European Research Council, Deutsche Krebshilfe, Von Behring-Röntgen-Stiftung, Deutsche José Carreras Leukämie Stiftung, and the Universities of Giessen and Marburg Lung Center (LOEWE).

Received: March 12, 2013
Revised: April 8, 2013
Accepted: April 8, 2013
Published: May 9, 2013

REFERENCES

Adams, J.M., Harris, A.W., Pinkert, C.A., Corcoran, L.M., Alexander, W.S., Cory, S., Palmiter, R.D., and Brinster, R.L. (1985). The c-myc oncogene driven by immunoglobulin enhancers induces lymphoid malignancy in transgenic mice. Nature *318*, 533–538.

Beckerman, R., and Prives, C. (2010). Transcriptional regulation by p53. Cold Spring Harb. Perspect. Biol. *2*, a000935.

Bensaad, K., Tsuruta, A., Selak, M.A., Vidal, M.N., Nakano, K., Bartrons, R., Gottlieb, E., and Vousden, K.H. (2006). TIGAR, a p53-inducible regulator of glycolysis and apoptosis. Cell *126*, 107–120.

Brady, C.A., Jiang, D., Mello, S.S., Johnson, T.M., Jarvis, L.A., Kozak, M.M., Kenzelmann Broz, D., Basak, S., Park, E.J., McLaughlin, M.E., et al. (2011). Distinct p53 transcriptional programs dictate acute DNA-damage responses and tumor suppression. Cell *145*, 571–583.

Bullock, A.N., and Fersht, A.R. (2001). Rescuing the function of mutant p53. Nat. Rev. Cancer *1*, 68–76.

Clarke, A.R., Purdie, C.A., Harrison, D.J., Morris, R.G., Bird, C.C., Hooper, M.L., and Wyllie, A.H. (1993). Thymocyte apoptosis induced by p53-dependent and independent pathways. Nature *362*, 849–852.

Collado, M., Gil, J., Efeyan, A., Guerra, C., Schuhmacher, A.J., Barradas, M., Benguría, A., Zaballos, A., Flores, J.M., Barbacid, M., et al. (2005). Tumour biology: senescence in premalignant tumours. Nature *436*, 642.

Cosme-Blanco, W., Shen, M.F., Lazar, A.J., Pathak, S., Lozano, G., Multani, A.S., and Chang, S. (2007). Telomere dysfunction suppresses spontaneous tumorigenesis in vivo by initiating p53-dependent cellular senescence. EMBO Rep. *8*, 497–503.

Crighton, D., Wilkinson, S., O'Prey, J., Syed, N., Smith, P., Harrison, P.R., Gasco, M., Garrone, O., Crook, T., and Ryan, K.M. (2006). DRAM, a p53-induced modulator of autophagy, is critical for apoptosis. Cell *126*, 121–134.

Dehner, A., Klein, C., Hansen, S., Müller, L., Buchner, J., Schwaiger, M., and Kessler, H. (2005). Cooperative binding of p53 to DNA: regulation by protein-protein interactions through a double salt bridge. Angew. Chem. Int. Ed. Engl. *44*, 5247–5251.

Demidov, O.N., Timofeev, O., Lwin, H.N., Kek, C., Appella, E., and Bulavin, D.V. (2007). Wip1 phosphatase regulates p53-dependent apoptosis of stem cells and tumorigenesis in the mouse intestine. Cell Stem Cell *1*, 180–190.

Deng, C., Zhang, P., Harper, J.W., Elledge, S.J., and Leder, P. (1995). Mice lacking p21CIP1/WAF1 undergo normal development, but are defective in G1 checkpoint control. Cell *82*, 675–684.

Donehower, L.A., Harvey, M., Slagle, B.L., McArthur, M.J., Montgomery, C.A., Jr., Butel, J.S., and Bradley, A. (1992). Mice deficient for p53 are developmentally normal but susceptible to spontaneous tumours. Nature *356*, 215–221.

García-Cao, I., García-Cao, M., Martín-Caballero, J., Criado, L.M., Klatt, P., Flores, J.M., Weill, J.C., Blasco, M.A., and Serrano, M. (2002). "Super p53" mice exhibit enhanced DNA damage response, are tumor resistant and age normally. EMBO J. *21*, 6225–6235.

Gottlieb, E., and Vousden, K.H. (2010). p53 regulation of metabolic pathways. Cold Spring Harb. Perspect. Biol. *2*, a001040.

Hermeking, H., and Eick, D. (1994). Mediation of c-Myc-induced apoptosis by p53. Science *265*, 2091–2093.

Hu, W., Zhang, C., Wu, R., Sun, Y., Levine, A., and Feng, Z. (2010). Glutaminase 2, a novel p53 target gene regulating energy metabolism and antioxidant function. Proc. Natl. Acad. Sci. USA *107*, 7455–7460.

Jacks, T., Remington, L., Williams, B.O., Schmitt, E.M., Halachmi, S., Bronson, R.T., and Weinberg, R.A. (1994). Tumor spectrum analysis in p53-mutant mice. Curr. Biol. *4*, 1–7.

Jeffers, J.R., Parganas, E., Lee, Y., Yang, C., Wang, J., Brennan, J., MacLean, K.H., Han, J., Chittenden, T., Ihle, J.N., et al. (2003). Puma is an essential mediator of p53-dependent and -independent apoptotic pathways. Cancer Cell *4*, 321–328.

Jiang, D., Brady, C.A., Johnson, T.M., Lee, E.Y., Park, E.J., Scott, M.P., and Attardi, L.D. (2011). Full p53 transcriptional activation potential is dispensable for tumor suppression in diverse lineages. Proc. Natl. Acad. Sci. USA *108*, 17123–17128.

Jones, R.G., Plas, D.R., Kubek, S., Buzzai, M., Mu, J., Xu, Y., Birnbaum, M.J., and Thompson, C.B. (2005). AMP-activated protein kinase induces a p53-dependent metabolic checkpoint. Mol. Cell *18*, 283–293.

Kitayner, M., Rozenberg, H., Kessler, N., Rabinovich, D., Shaulov, L., Haran, T.E., and Shakked, Z. (2006). Structural basis of DNA recognition by p53 tetramers. Mol. Cell *22*, 741–753.

Labi, V., Erlacher, M., Krumschnabel, G., Manzl, C., Tzankov, A., Pinon, J., Egle, A., and Villunger, A. (2010). Apoptosis of leukocytes triggered by acute DNA damage promotes lymphoma formation. Genes Dev. *24*, 1602–1607.

Li, T., Kon, N., Jiang, L., Tan, M., Ludwig, T., Zhao, Y., Baer, R., and Gu, W. (2012). Tumor suppression in the absence of p53-mediated cell-cycle arrest, apoptosis, and senescence. Cell *149*, 1269–1283.

Liu, G., Parant, J.M., Lang, G., Chau, P., Chavez-Reyes, A., El-Naggar, A.K., Multani, A., Chang, S., and Lozano, G. (2004). Chromosome stability, in the absence of apoptosis, is critical for suppression of tumorigenesis in Trp53 mutant mice. Nat. Genet. *36*, 63–68.

Lowe, S.W., Ruley, H.E., Jacks, T., and Housman, D.E. (1993a). p53-dependent apoptosis modulates the cytotoxicity of anticancer agents. Cell *74*, 957–967.

Lowe, S.W., Schmitt, E.M., Smith, S.W., Osborne, B.A., and Jacks, T. (1993b). p53 is required for radiation-induced apoptosis in mouse thymocytes. Nature *362*, 847–849.

Lowe, S.W., Bodis, S., McClatchey, A., Remington, L., Ruley, H.E., Fisher, D.E., Housman, D.E., and Jacks, T. (1994). p53 status and the efficacy of cancer therapy in vivo. Science *266*, 807–810.

Martins, C.P., Brown-Swigart, L., and Evan, G.I. (2006). Modeling the therapeutic efficacy of p53 restoration in tumors. Cell *127*, 1323–1334.

Matoba, S., Kang, J.G., Patino, W.D., Wragg, A., Boehm, M., Gavrilova, O., Hurley, P.J., Bunz, F., and Hwang, P.M. (2006). p53 regulates mitochondrial respiration. Science *312*, 1650–1653.

Michalak, E.M., Villunger, A., Adams, J.M., and Strasser, A. (2008). In several cell types tumour suppressor p53 induces apoptosis largely via Puma but Noxa can contribute. Cell Death Differ. *15*, 1019–1029.

Olive, K.P., Tuveson, D.A., Ruhe, Z.C., Yin, B., Willis, N.A., Bronson, R.T., Crowley, D., and Jacks, T. (2004). Mutant p53 gain of function in two mouse models of Li-Fraumeni syndrome. Cell *119*, 847–860.

Reimann, M., Lee, S., Loddenkemper, C., Dörr, J.R., Tabor, V., Aichele, P., Stein, H., Dörken, B., Jenuwein, T., and Schmitt, C.A. (2010). Tumor stroma-derived TGF-beta limits myc-driven lymphomagenesis via Suv39h1-dependent senescence. Cancer Cell *17*, 262–272.

Reinhardt, H.C., and Schumacher, B. (2012). The p53 network: cellular and systemic DNA damage responses in aging and cancer. Trends Genet. *28*, 128–136.

Sablina, A.A., Budanov, A.V., Ilyinskaya, G.V., Agapova, L.S., Kravchenko, J.E., and Chumakov, P.M. (2005). The antioxidant function of the p53 tumor suppressor. Nat. Med. *11*, 1306–1313.

Schlereth, K., Beinoraviciute-Kellner, R., Zeitlinger, M.K., Bretz, A.C., Sauer, M., Charles, J.P., Vogiatzi, F., Leich, E., Samans, B., Eilers, M., et al. (2010a). DNA binding cooperativity of p53 modulates the decision between cell-cycle arrest and apoptosis. Mol. Cell *38*, 356–368.

Schlereth, K., Charles, J.P., Bretz, A.C., and Stiewe, T. (2010b). Life or death: p53-induced apoptosis requires DNA binding cooperativity. Cell Cycle *9*, 4068–4076.

Schmitt, C.A., Fridman, J.S., Yang, M., Baranov, E., Hoffman, R.M., and Lowe, S.W. (2002). Dissecting p53 tumor suppressor functions in vivo. Cancer Cell *1*, 289–298.

Serrano, M., Lin, A.W., McCurrach, M.E., Beach, D., and Lowe, S.W. (1997). Oncogenic ras provokes premature cell senescence associated with accumulation of p53 and p16INK4a. Cell *88*, 593–602.

Shreeram, S., Demidov, O.N., Hee, W.K., Yamaguchi, H., Onishi, N., Kek, C., Timofeev, O.N., Dudgeon, C., Fornace, A.J., Anderson, C.W., et al. (2006). Wip1 phosphatase modulates ATM-dependent signaling pathways. Mol. Cell *23*, 757–764.

Suzuki, S., Tanaka, T., Poyurovsky, M.V., Nagano, H., Mayama, T., Ohkubo, S., Lokshin, M., Hosokawa, H., Nakayama, T., Suzuki, Y., et al. (2010). Phosphate-activated glutaminase (GLS2), a p53-inducible regulator of glutamine metabolism and reactive oxygen species. Proc. Natl. Acad. Sci. USA *107*, 7461–7466.

Toledo, F., Krummel, K.A., Lee, C.J., Liu, C.W., Rodewald, L.W., Tang, M., and Wahl, G.M. (2006). A mouse p53 mutant lacking the proline-rich domain rescues Mdm4 deficiency and provides insight into the Mdm2-Mdm4-p53 regulatory network. Cancer Cell *9*, 273–285.

Van Nguyen, T., Puebla-Osorio, N., Pang, H., Dujka, M.E., and Zhu, C. (2007). DNA damage-induced cellular senescence is sufficient to suppress tumorigenesis: a mouse model. J. Exp. Med. *204*, 1453–1461.

Ventura, A., Kirsch, D.G., McLaughlin, M.E., Tuveson, D.A., Grimm, J., Lintault, L., Newman, J., Reczek, E.E., Weissleder, R., and Jacks, T. (2007). Restoration of p53 function leads to tumour regression in vivo. Nature *445*, 661–665.

Vousden, K.H., and Prives, C. (2009). Blinded by the light: the growing complexity of p53. Cell *137*, 413–431.

Xue, W., Zender, L., Miething, C., Dickins, R.A., Hernando, E., Krizhanovsky, V., Cordon-Cardo, C., and Lowe, S.W. (2007). Senescence and tumour clearance is triggered by p53 restoration in murine liver carcinomas. Nature *445*, 656–660.

Yoon, K.A., Nakamura, Y., and Arakawa, H. (2004). Identification of ALDH4 as a p53-inducible gene and its protective role in cellular stresses. J. Hum. Genet. *49*, 134–140.